Molecular Therapy
Oncolytics
Original Article

PI3K-activated MSC proteomes inhibit mammary tumors via Hsp90ab1 and Myh9

Xun Sun,[1,2,6] Kexin Li,[1,2,6] Uma K. Aryal,[3] Bai-Yan Li,[1] and Hiroki Yokota[1,2,4,5]

[1]Department of Pharmacology, School of Pharmacy, Harbin Medical University, Harbin 150081, China; [2]Department of Biomedical Engineering, Indiana University Purdue University Indianapolis, Indianapolis, IN 46202, USA; [3]Department of Comparative Pathobiology, Purdue University, West Lafayette, IN 47907, USA; [4]Indiana Center for Musculoskeletal Health, Indianapolis, IN 46202, USA; [5]Simon Cancer Center, Indiana University School of Medicine, Indianapolis, IN 46202, USA

Despite the advance in medications in the past decade, aggressive breast cancer such as triple-negative breast cancer is difficult to treat. Here, we examined a counter-intuitive approach to converting human bone marrow-derived mesenchymal stem cells (MSCs) into induced tumor-suppressing cells by administering YS49, a PI3K/Akt activator. Notably, PI3K-activated MSCs generated tumor-suppressive proteomes, while PI3K-inactivated MSCs tumor-promotive proteomes. In a mouse model, the daily administration of YS49-treated MSC-derived CM decreased the progression of primary mammary tumors as well as the colonization of tumor cells in the lung. In the *ex vivo* assay, the size of freshly isolated human breast cancer tissues, including estrogen receptor positive and negative as well as human epidermal growth factor receptor 2 (HER2) positive and negative, was decreased by YS49-treated MSC-derived CM. Hsp90ab1 was enriched in CM as an atypical tumor-suppressing protein and immunoprecipitated a non-muscle myosin, Myh9. Extracellular Hsp90ab1 and Myh9 exerted the anti-tumor action and inhibited the maturation of bone-resorbing osteoclasts. Collectively, this study demonstrated that the activation of PI3K generated tumor-suppressive proteomes in MSCs and supported the possibility of using patient-derived MSCs for the treatment of breast cancer and bone metastasis.

INTRODUCTION

As Newton's third law of motion indicates, an opposite reaction for every action and Darwin's law of natural selection necessitates a survival-of-the-fittest competition, many cancer cells tend to develop resistance to chemotherapeutic agents in a ferocious environment. In exploring a novel therapeutic option for advanced cancer, we evaluated a counter-intuitive, yet rational strategy by considering the reversed reaction and a survival-of-the-fittest rivalry of cancer cells. Here, we reported converting mesenchymal stem cells (MSCs) into tumor-suppressive cells by activating oncogenic signaling, using breast cancer and bone metastasis as a model system. In the United States, breast cancer is the most frequently diagnosed cancer for women and approximately 13% of U.S. women succumb to invasive breast cancer in their lifetime. The death rates in the United States are the highest among all cancers except for lung cancer, because of its metastases to other organs such as the lungs, brain, and bones.[1,2]

To prevent the progression of primary tumors as well as tumor-induced bone destruction, we have previously developed a counter-intuitive approach to convert osteocytes, MSCs, and even tumor cells into tumor-suppressing cells.[3–5] Paradoxically, tumorigenic pathways such as Wnt and PI3K/Akt signaling were activated in host cells that generated tumor-suppressive, bone-protective proteomes. We named those engineered cells induced tumor-suppressing cells (iTSCs) and applied their conditioned medium (CM) for preventing tumor progression and tumor-induced bone loss.[6]

Cancer cell secretomes contain varying signals from cancer cells to the extracellular domain. They generally promote tumor progression and metastasis through varying mechanisms, such as metabolic alterations and immunosuppression.[7] Diagnostic and prognostic biomarkers can be identified in the secretomes since they can build a tumor microenvironment and induce chemoresistance.[8–10] For instance, it is reported that the application of doxorubicin enriches oncogenic proteins in the secretomes.[11] It is recently reported that cancer cells release succinate, a key intermediate in metabolism, that can promote tumor progression and metastasis.[12] Besides soluble biomolecules, including signaling factors, cytokines, and other metabolites, the secretomes also include exosomes with varying RNA components.[13] One caution in interpreting the role of cancer cell secretomes is context dependence. Our group has shown that proteins such as a heat shock protein, Hsp90ab1, act as a tumor promoter intracellularly and a tumor suppressor extracellularly.[5] By contrast, high mobility group box protein 1 is known to serve as a tumor suppressor in the cytoplasm and a tumor promoter in the extracellular domain.[14]

The generation of iTSCs resembles cell competition during the organogenesis of *Drosophila melanogaster*, where mutant less-fit cells are

Received 21 February 2022; accepted 2 August 2022;
https://doi.org/10.1016/j.omto.2022.08.003.

[6]These authors contributed equally

Correspondence: Bai-Yan Li, MD, PhD, Department of Pharmacology, School of Pharmacy, Harbin Medical University, #157 Baojian Road, Harbin 150081, China.
E-mail: liby@ems.hrbmu.edu.cn
Correspondence: Hiroki Yokota, PhD, Department of Biomedical Engineering, Indiana U. Purdue U. Indianapolis, 723 West Michigan Street, Indianapolis, IN 46202 USA.
E-mail: hyokota@iupui.edu

eliminated by wild-type cells.[15] For instance, cells in a *Drosophila* eye disc with higher protein synthesis are reported to eliminate their neighboring cells with lower fitness.[16] Cell culture studies also support the presence of secreted signals that mediate cell competition.[17] As a novel option for cancer treatment, we developed iTSCs as cells with higher fitness and applied their CM to inhibit tumor progression. The anti-tumor action of CM was resistant to nuclease treatment and filtering with a 3-kD cutoff, and we thus focused on the proteomes as anti-tumor agents.[18] Since the previous work was mainly conducted using mouse cells, the question herein was whether human-derived MSCs, which have been used in regenerative medicine and can be harvested from bone marrow,[19] would be used to generate iTSCs and tumor-suppressive proteomes. We examined commercially available human MSCs, as well as adherent cells isolated from a human bone marrow aspirate-derived MSC (BMSCs). While MSCs have been shown to promote tumor progression and metastases,[20,21] it is also reported that they could inhibit tumor growth by secreting soluble factors.[22,23]

Besides testing the anti-tumor capability of iTSCs using *in vitro* systems and a mouse model, we applied BMSC-derived CM to freshly isolated human breast cancer tissues. This *ex vivo* assay is a precursor to a clinical trial. Because of the potential dependence of anti-tumor efficacy on the types of hormonal receptors, we used both estrogen receptor (ER)-positive and negative as well as human epidermal growth factor receptor 2 (HER2) positive and negative. We also used human breast-derived epithelial cells as non-tumor control cells and evaluated tumor-selective inhibition of PI3K-activated CM.

In iTSC CMs in our previous studies, a group of well-known tumor-suppressing proteins, such as p53 and Trail, as well as atypical tumor suppressors such as polyubiquitin C, enolase 1, moesin, and Hsp90ab1 (Hsp90beta), have been identified and characterized.[4,6] The latter group of tumor-suppressing proteins is mostly moonlighting, and their anti- and pro-tumorigenic actions depend on their extracellular and intracellular locations. For instance, the overexpression of Lrp5, a Wnt coreceptor, in breast cancer cells is reported to enhance tumorigenic phenotypes, whereas its overexpression in osteocytes strengthens the anti-tumor action of osteocytes.[5] Although multiple lines of evidence support a tumorigenic role of Hsp90ab1,[24] we evaluated its paradoxical, anti-tumor action in the extracellular domain. Using the proteins that were coimmunoprecipitated with Hsp90ab1, we conducted mass spectrometry-based whole-genome proteomics. While Hsp90ab1 is a molecular chaperone that stabilizes client proteins, it is often upregulated in cancer cells and their level correlates with malignancy.[25] It has been shown that extracellular Hsp90ab1, secreted from osteosarcoma cells, inhibits the activation of latent transforming growth factor (TGF) β.[26] Furthermore, it has multiple binding partners and assists their structural integrity.[27] The mass spectrometry-based proteomics analysis in this study revealed its interactions with cytoskeletal proteins such as tubulin, actin, and myosin, as well as other heat shock proteins (Hsp90aa1, Hspa8).

In this study, we evaluated the role of extracellular myosin and actin, cytoskeletal elements, in the tumor-suppressive proteomes. Myosins compose of a superfamily of motor proteins that are responsible for actin-based motility. They are also involved in various tumorigenic processes, including cell adhesion, cell migration, cytokinesis, and cell polarity.[28] In this study, Hsp90ab1 co-immunoprecipitated myosin heavy chain 9 (Myh9), which generates non-muscle myosin II.[29] While Myh9 is known to act as a tumor suppressor in head and neck and skin tumors, it is also shown to behave as an oncogene in other solid tumors.[30] A high level of Myh9 is also reported in many malignant tumors, including breast cancer and leukemia. We observed that extracellular Myh9 served as a tumor suppressor together with Hsp90ab1 in triple-negative breast cancer, as well as the inhibitor of bone-resorbing osteoclasts. Collectively, the results shed new insight into the anti-tumor action of PI3K-activated MSCs with multi-tasking Hsp90ab1 and Myh9.

RESULTS

Tumor-suppressing effects of YS49 MSC-derived CM

Human MSCs were treated with 20 μM YS49 for 1 day, and the anti-tumor capability of their CM was examined. The result with MDA-MB-231 breast cancer cells revealed that YS49 MSC CM reduced MTT-based viability, EdU-based proliferation, scratch-based motility, and transwell invasion (Figures 1A–1D). The decrease in MTT-based viability, EdU-based proliferation, and transwell invasion was also observed in MDA-MB-436 breast cancer cells (Figures 1E–1G) and MCF7 breast cancer cells (Figure S1).

We also used a bone marrow aspirate from a healthy individual. Cells were suspended in a culture medium and adherent cells were collected as BMSCs. Of note, BMSCs included all adherent cells such as fibroblasts, macrophages, and endothelial progenitor cells. BMSCs were treated with 20 μM YS49 and the anti-tumor capability of their CM (YS49 BMSC CM) was examined. The results were consistent with the MSC results. In MDA-MB-231 cells, YS49 BMSC CM decreased EdU-based proliferation, as well as transwell invasion (Figures2A and 2B). Furthermore, it decreased the ability of metabolic activity, proliferation, and invasion of MDA-MB-436 cells (Figures 2C–2E) and MCF7 breast cancer cells (Figure S2). Besides treatment with YS49, the overexpression of Akt in BMSCs also induced the anti-tumor effects to MDA-MB-231 cells (Figure S3).

Tumor-promoting effects or undetectable tumor-suppressing effects of BKM120-treated MSC/BMSC-derived CM

While YS49-derived MSC/BMSC CM showed tumor-suppressing effects, the effects of BKM120, a PI3K inhibitor, did not present any anti-tumor actions. Notably, BKM120-treated MSC-derived CM promoted MTT-based viability, EdU-based proliferation, scratch-based motility, and transwell invasion of MDA-MB-231 cells. Also, BKM120-treated BMSC-derived CM promoted the viability and proliferation of MDA-MB-231 cells, and any changes were undetectable in scratch-based motility and transwell invasion (Figures 3A–3D). No significant effect was observed in MDA-MB-436 cells by BKM120-treated MSC/BMSC CM (Figures 3E and 3F).

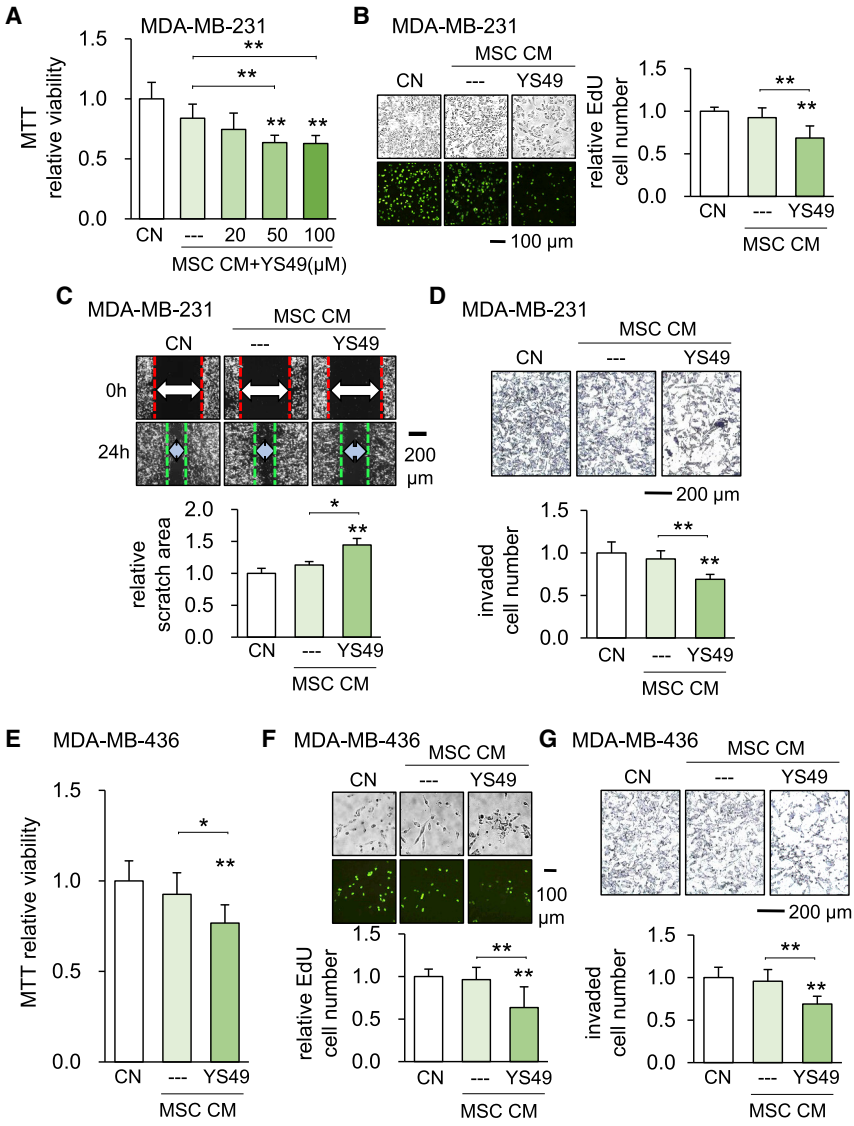

Figure 1. Tumor-suppressing effects of YS49-treated MSC-derived CM (YS49 MSC CM)

CN, control. *p < 0.05 and **p < 0.01. (A–D) Reduction in MTT viability, EdU cell proliferation, scratch-based motility, and cross-membrane invasion of MDA-MB-231 breast cancer cells by YS49 MSC CM. (E–G) Reduction in MTT metabolic activity, EdU cell proliferation, and cross-membrane invasion of MDA-MB-436 cells by YS49 MSC CM.

Tumor-suppressing capability *in vivo* by YS49-treated MSC/BMSC-derived CM

We next evaluated the effect of the application of YS49-treated MSC/BMSC CM on mammary tumors and lung metastasis. In the NSG female mouse model, the 2-week daily intravenous injection of YS49-treated MSC/BMSC CM from the tail vein significantly decreased the size and weight of mammary tumors (Figure 4A).

We also examined the suppressive effect on the tumor invasion. Using NSG female mice, MDA-MB-231 cells were introduced via intra-cardiac injection and their invasion to the lung was histologically examined. While a significant number of tumor cells were detected in the lung of the placebo group, the daily YS49 CM injection for 3 weeks substantially decreased the size of tumor-invaded lung areas (Figure 4B).

Tumor selectivity

We have so far shown that YS49 CM presents tumor-suppressive capabilities for primary mammary tumors as well as secondary invasion to the lung. We next examined the effect of these CMs on non-cancer epithelial cells *in vitro*. Here, we defined tumor selectivity as the ratio of the reduction of MTT viability between tumor and non-tumor cells. If the ratio is greater than 1, the inhibition is selective to tumor cells compared with non-tumor cells. Using two breast cancer cell lines (MDA-MB-231 and 436) and two non-cancer epithelial cells of breast origin (KTB6-hTERT and KTB34-hTERT), we observed that the tumor selectivity was greater than 1 with YS49 MSC/BMSC CM (Figures 4C and 4D), indicating that CM's inhibitory effects were selective to tumor cells.

Inhibition of osteoclast development

In addition to the capability of tumor suppression, we further examined the effect of YS49 CM on the development of bone-resorbing osteoclasts. In bone metastasis associated with breast cancer, mature osteoclasts play a major role in tumor-induced osteolysis. The treatment of RAW264.7 pre-osteoclasts with 40 ng/mL RANKL stimulated the formation of multinucleated mature osteoclasts in 4 days (Figures 5A and 5B). However, their incubation with YS49 MSC/BMSC CM inhibited the development of multinucleated mature osteoclasts. Of note, CM without YS49 treatment did not alter the fate of osteoclasts. Consistently, YS49 MSC/BMSC CM decreased the level of NFATc1, a critical transcription factor in osteoclast differentiation, as well as cathepsin K, a proteinase that plays a pivotal role in osteoclast-mediated bone resorption (Figures 5C and 5D). By contrast, BKM120-treated MSC/BMSC CM did not show an inhibitory effect (Figures 5E and 5F).

Shrinkage of human breast cancer fragments by YS49 CM

So far, *in vitro* and *in vivo* results support the suppression of tumor progression and invasion, as well as bone resorption using triple-negative breast cancer cells and pre-osteoclasts. We then tested the effect of YS49 CM on the growth of freshly isolated human breast

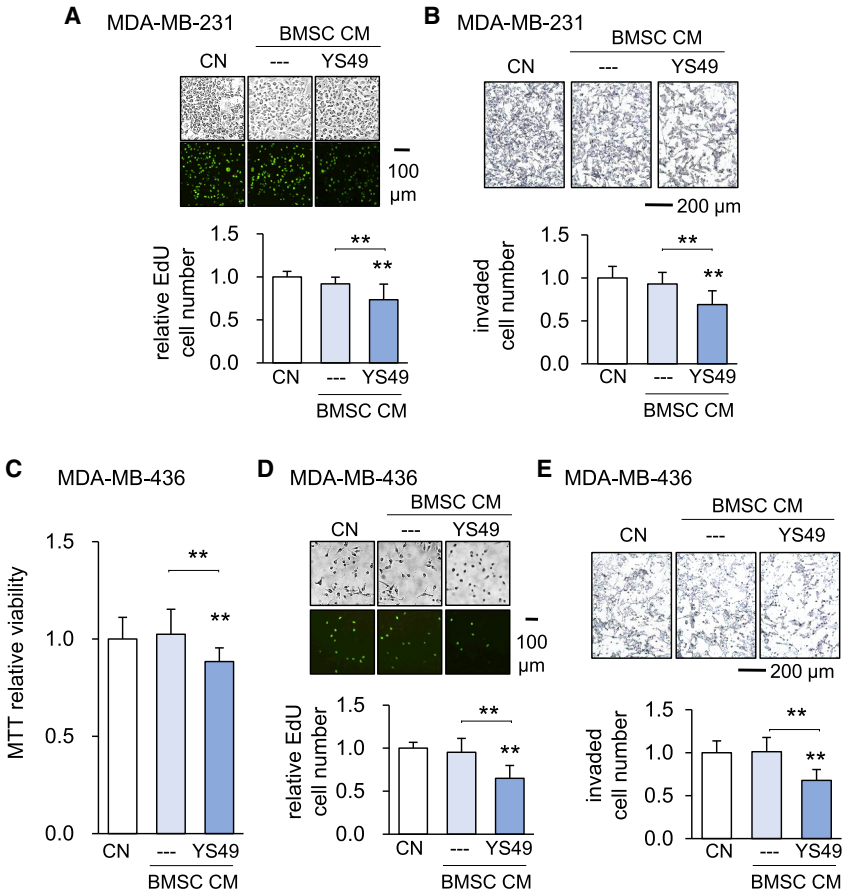

Figure 2. Tumor-suppressing effects of YS49-treated bone marrow MSC-derived CM (YS49 BMSC CM)

(A, B) Reduction in EdU cell proliferation, and cross-membrane invasion of MDA-MB-231 cells by YS49 BMSC CM. (C–E) Reduction in MTT viability, EdU proliferation, and transwell invasion of MDA-MB-436 cells by YS49 BMSC CM. CN, control. **p < 0.01.

cancer tissues *ex vivo*. Four different tissues (ER+/PR+/HER–, ER+/PR–/HER–, ER–/PR+/HER+, and ER–/PR–/HER+) were incubated in two YS49 CMs, derived from MSCs and BMSCs. These tissues included both ER positive and negative and HER2 positive and negative. Notably, regardless of the selected hormonal receptor status, the size of all tissue fragments was significantly decreased after 96 h (Figures 6A–6D).

Hsp90ab1 and myosin 9 as tumor suppressors

In our previous study, Hsp90ab1 was identified as one of the most influential tumor suppressors in Akt-overexpressed MSC-derived CM.[5] Using mass spectrometry-based proteomics analyses, we thus focused on the identification of its partner proteins using immunoprecipitation. Since Hsp90ab1 acted as a tumor suppressor in the extracellular matrix (ECM) domain, we focused on the proteins mostly located in the ECM of MDA-MB-231 breast cancer cells. Of note, the protein extract we used also contained cytoplasmic proteins that were derived from damaged cells during protein collection. Of 1,597 proteins identified by mass spectrometry, a short list of 13 proteins, whose relative abundance score was greater than 50, was selected (Figure 7A). A list of 64 proteins, whose score was greater than 20, was also provided (Table S1). On the short list, three major groups of proteins were included, such as heat shock proteins (Hsp90aa1 and Hspa8), previously identified tumor-suppressor proteins in iTSCs (Eef2 and Eno1),[3] and skeletal proteins (Actb, tubb4d, and Myh9). In this study, we evaluated the role of Actb (β-actin) and Myh9 (myosin 9) in tumor progression because of their potential linkage to ECM.

Western blotting confirmed that β-actin and Myh9 immunoprecipitated with Hsp90ab1 (Figure 7B). We observed that recombinant Myh9 proteins acted as a tumor suppressor and reduced viability, proliferation, 2-dimensional motility, and invasion of MDA-MB-231 breast cancer cells (Figures 7C–7F). Interestingly, Myh9 and Hsp90ab1 also inhibited the multinucleation of RANKL-stimulated RAW264.7 preosteoclasts and deregulated NFATc1 and cathepsin K (Figures 7G and 7H). By contrast, Actb did not show any detectable tumor-suppressive capabilities (Figures 7C–7F).

Hsp90ab1 and Myh9 at 1–10 μg/mL acted as potent tumor suppressors in a dose-dependent fashion and their tumor-suppressive effect was additive (Figures 8A and 8B). Notably, the tumor-suppressive effect of Hsp90ab1 was not suppressed by silencing Myh8 in MDA-MB-231 and -436 breast cancer cells, indicating that Myh9 in tumor cells did not mediate Hsp90ab1-driven anti-tumor ability (Figure 8C). Since Myh9 was not detected in iTSC CM (Figure S4A), the result suggests that Myh9 in the ECM contributes to the suppression of tumor progression. The ELISA-based concentrations of Myh9 in the ECM-enriched protein extract of MDA-MB-231 and 436 breast cancer cells are shown (Figure S4B).

DISCUSSION

This study presented that human MSCs and bone marrow aspirate-derived MSCs (BMSCs) can be used to generate iTSCs by activating PI3K/Akt signaling with a pharmacological agent, YS49. YS49 CM acted as tumor-suppressive proteomes and decreased the proliferation, migration, and invasion of MDA-MB-231 and 436 breast cancer cells. It also decreased the size of freshly isolated breast cancer tissues with four different hormonal receptor types.[31] Furthermore, YS49 CM suppressed the progression of mammary tumors and the tumor colonization in the lung of NSG mice. Collectively, this study showed

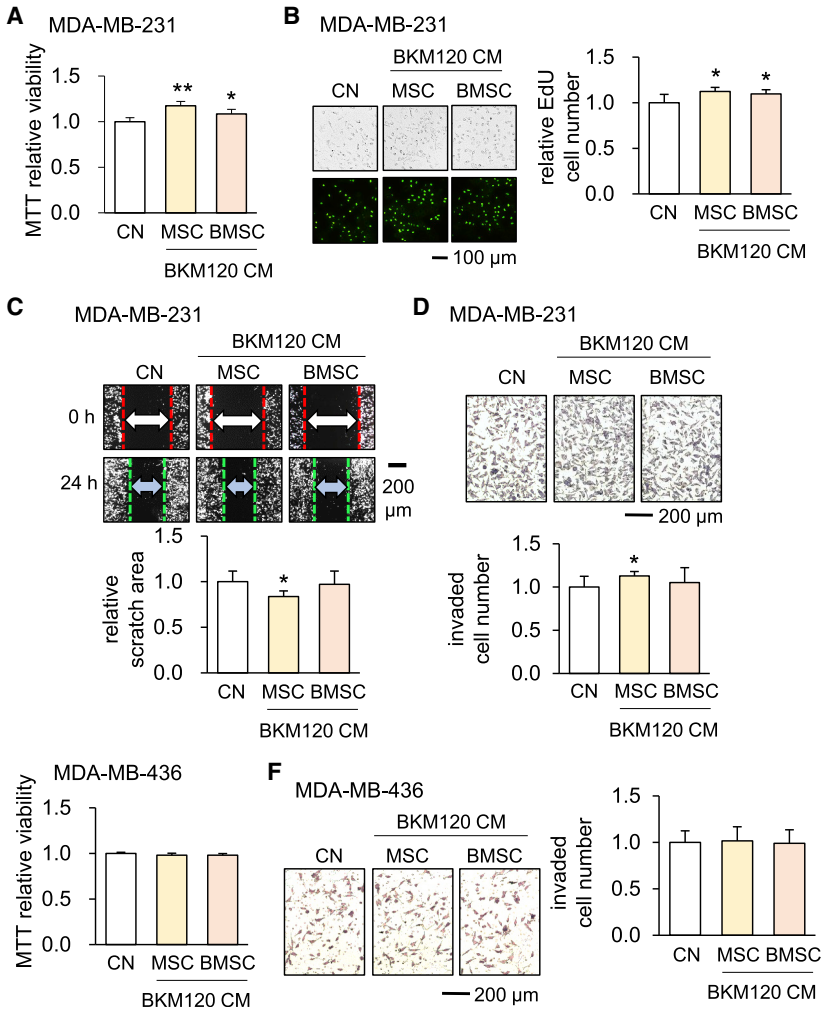

Figure 3. Tumor-promoting or no detectable effects by BKM120-treated MSC/BMSC-derived CM

(A–D) Increase in MTT viability, EdU cell proliferation, two-dimensional motility, and cross-membrane invasion of MDA-MB-231 cells in response to BKM120 MSC CM, as well as the promotion of MTT viability and EdU cell proliferation in MDA-MB-231 breast cells in response to BKM120 BMSC CM. (E–F) No significant effect in MTT viability and transwell invasion of MDA-MB-436 cells by BKM120 MSC/BMSC CM. CN, control. *$p < 0.05$ and **$p < 0.01$.

for the first time the possibility of developing iTSCs and their tumor-suppressive proteome from the bone marrow aspirate of a patient with breast cancer.

In our previous studies using osteocytes, MSCs, and cancer cells in the breast, prostate, and pancreas, we generated iTSCs by overexpressing β-catenin and Lrp5 in Wnt signaling.[4,5] The whole-genome proteomics analyses predicted a list of atypical tumor-suppressing protein candidates. Extracellular Hsp90ab1 was one of the tumor-suppressing proteins frequently enriched in those iTSC CMs, together with enolase 1, moesin, and ubiquitin C.[3,32] Interestingly, many of them function as tumor suppressors in the extracellular domain, while they serve as tumor promoters in the intracellular domain. Hsp90ab1 and Hsp90aa1 are evolutionarily conserved molecular chaperones in the Hsp90 family,[33] and they are present in the extracellular domain and exosomes.[34] It is reported that Hsp90ab1 suppresses the production of active TGFβ, which stimulates tumor-induced osteolysis.[26,32] We have shown that small molecules such as dopamine act as tumor suppressors.[18] However, we also observed that filtering CM with a 3-kD cutoff filter, the treatment with nucleases, and the ultracentrifugation for removing microparticles and exosomes did not significantly alter CM's anti-tumor actions.[35]

The immunoprecipitation assay, followed by whole-genome proteomics, revealed that Hsp90ab1 immunoprecipitated Myh9, a non-muscle myosin. Myh9 is a heavy chain of non-muscle myosin IIA, an extensively expressed myosin, which generates intracellular chemo-mechanical force and translocates actin filaments.[29] Both Hsp90ab1 and Myh9 are moonlighting proteins, whose anti- and pro-tumorigenic functions differ depending on context. They may act as tumor-promoting proteins when present in the intracellular domain,[24,36,37] whereas extracellular Hsp90ab1 and Myh9 interacted and their recombinant proteins in the culture medium suppressed the tumorigenic behaviors of cancer cells. The role of Hsp90ab1-Myh9 interaction needs to be further clarified for suppressing tumor progression. Hsp90ab1 may stabilize extracellular Myh9 as a molecular chaperone and indirectly assist the anti-tumor action of Myh9. Alternatively, Hsp90ab1 may interact with Myh9 in ECM and may convert the micro ECM environment unfavorable for cancer progression. The anti-tumor effect of extracellular Hsp90ab1 and Myh9 was additive, and, based on RNA interference, Myh9 in tumor cells was not involved in Hsp90ab1-driven tumor suppression. Tumor cells tend to develop resistance to chemotherapeutic drugs.[38] It is recommended to examine whether the application of a protein cocktail, which consists of tumor-suppressing proteins in CM such as Hsp90ab1, may assist the tumor-suppressive action of existing chemotherapeutic agents and reduce chemoresistance development.

In addition to the suppression of tumor progression, we observed that extracellular Hsp90ab1and Myh9 inhibited the maturation of bone-resorbing osteoclasts. They also downregulated NFATc1 transcription factor and cathepsin K proteinase.[39,40] Since the osteolytic vicious cycle in breast cancer-associated bone metastasis is promoted

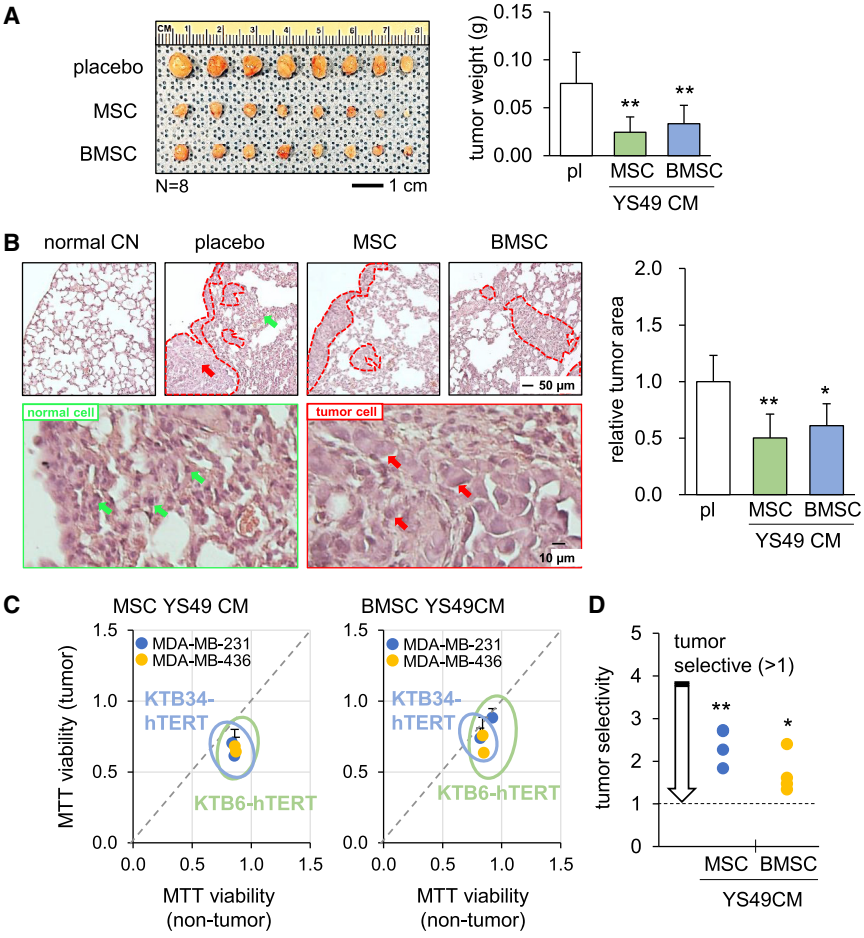

Figure 4. Suppression of primary tumors and lung metastasis in NSG female mice by YS49 MSC/BMSC CM

(A) Significant decrease in mammary tumor weight by YS49 MSC/BMSC CMs. n = 8. (B) Prevention of lung metastasis by YS49 MSC/BMSC CMs. n = 5. (C, D) Selective reduction in MTT viability of two cancer cell lines (MDA-MB-231 and 436) compared with non-cancer epithelial cells of breast origin (KTB6 and KTB34). Since the value of tumor selectivity (ratio of MTT values) is greater than 1, two CMs (MSC CM and BMSC CM) reduced the MTT-based metabolic activities of tumor cells more than those of non-tumor epithelial cells. Pl, placebo, CN, control. *p < 0.05 and **p < 0.01.

via tumor-osteoclast interactions, the suppression of osteoclast development by YS49 CM contributes to protecting tumor-driven bone loss.[41] The proposed mechanism of YS49 CM's tumor-suppressive, bone-protective action is depicted (Figure 8D).

While the concept of iTSCs was originated in the anti-tumor role of Wnt signaling in osteocytes,[4] the killing of neighboring cells by cells with enhanced protein synthesis has been reported as a process of cell competition in the organogenesis of *Drosophila*.[17] Cell competition is a combination of the elimination of unfit cells and the selection of fitter cells.[16] PI3K signaling is one of the most critical pathways to regulate protein synthesis, and we used the activation of PI3K signaling to generate iTSCs. An intriguing question is whether the activation of PI3K signaling is the most effective way to generate MSC-derived iTSCs. We envision that cell engineering may enable the conversion of MSCs into enhanced iTSCs with stronger tumor-suppressive proteomes than PI3K-activated MSCs.

MSCs are attractive candidates for regenerative medicine because of their potential for self-renewal and pluripotency, as well as their nutritional and immunosuppressive effects. MSCs undergoing extensive *in vitro* passage can undergo morphological, phenotypic and genetic changes. In regenerative medicine and bone fracture healing, patient-derived MSCs have been applied.[42] As a therapeutic tool for cancer treatment, the use of MSCs is listed in more than 200 studies at ClinicalTrials.gov in the U.S. in 2021. This study showed the possibility of generating tumor-suppressive proteomes using autologous MSCs for the treatment of breast cancer and associated metastases such as bone metastasis. In this studywe used commercially available MSCs as well as bone marrow-derived adherent cells as BMSCs. We have previously shown that macrophages and T lymphocytes, which can be derived from the peripheral blood, are converted into iTSCs.[6,18]Collectively, this study indicated the possibility of developing the MSC-derived iTSC-based therapeutic option.

This study demonstrated that iTSCs, derived from the human bone marrow aspirate, can generate the tumor-suppressive proteome. The proteome suppressed the proliferation, migration, and invasion of breast cancer cells and inhibited the maturation of bone-resorbing osteoclasts. The action of iTSC CM was at least in part regulated additively by extracellular Hsp90ab1 and Myh9, and they contributed to the selective inhibition of tumor cells over non-tumor cells. The results provide an unconventional option for developing pharmacological agents that effectively activate (not inhibit) PI3K signaling. The study also suggests the potential use of iTSCs and their CM for the treatment of breast cancer and associated metastasis using engineered MSCs derived from a patient with breast cancer.

MATERIALS AND METHODS

Cell culture and agents

MDA-MB-231, MDA-MB-436, and MCF-7 breast cancer cell lines (ATCC, Manassas, VA) were grown in RPMI-1640 (Gibco, Carlsbad, CA). Human MSCs (PT-2501, Lonza, Basel, Switzerland) and human bone marrow-derived MSCs (BMSCs; 1M-105, Lonza) were grown in

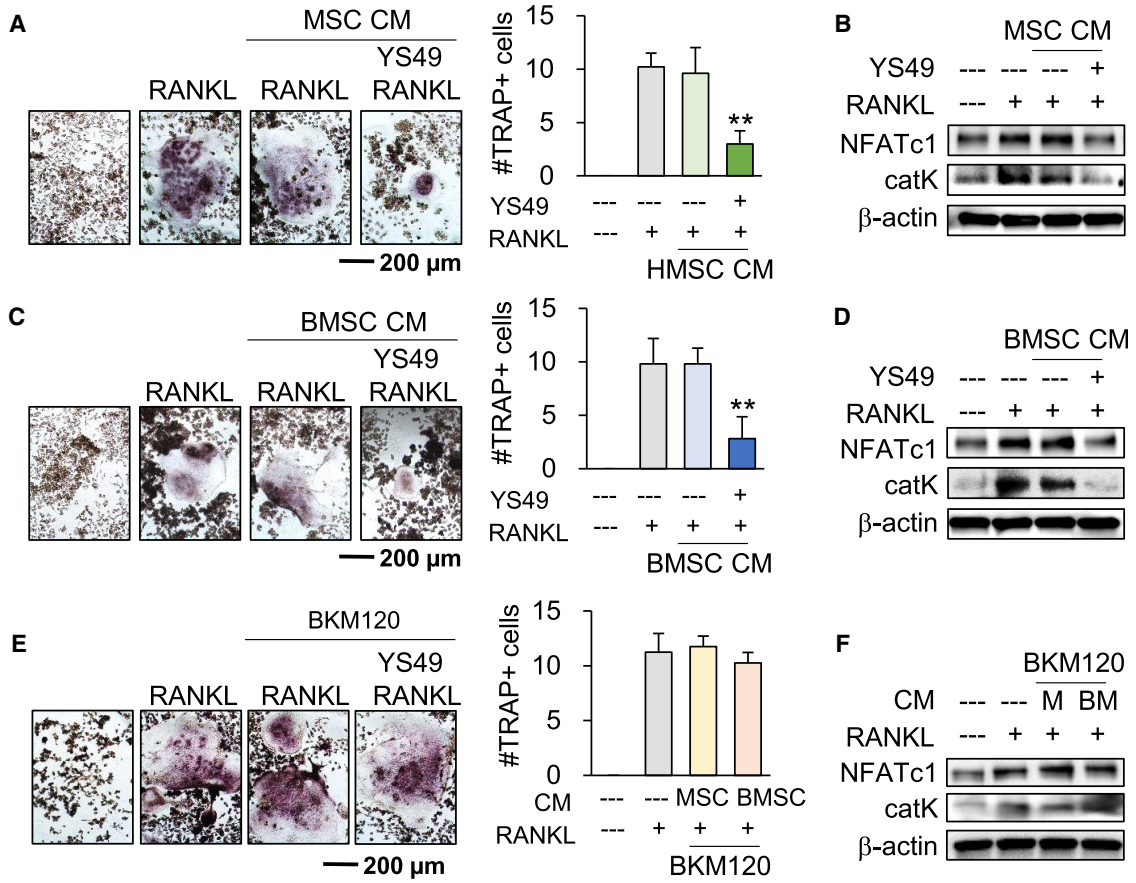

Figure 5. Inhibition of osteoclast development

(A, B) Reduction in the number of RANKL-stimulated multi-nucleated osteoclasts by YS49-treated MSC/BMSC-derived CM. (C, D) Reduction in NFATc1 and cathepsin K in RAW264.7 cells by YS49-treated MSC/BMSC-derived CM. *$p < 0.05$ and **$p < 0.01$. (E, F) No inhibition effect of osteoclast development by BKM120-treated MSC/BMSC CM.

MSCBM (PT-3001, Lonza), while αMEM was used to culture RAW264.7 pre-osteoclast cells (ATCC). As non-cancer control cells, we cultured human breast-derived epithelial cells (KTB6 and KTB34; obtained from Dr. Nakshatri, Indiana University, Bloomington, IN) in F12 and low glucose DMEM (3:1), which was supplemented with 5 μg/mL insulin (I5500, Sigma, St. Louis, MO,), 0.4 μg/mL hydrocortisone (H0888, Sigma), and 20 ng/mL EGF (236-EG-200, R&D Systems, Minneapolis, MN).[43] Cells were grown with 10% fetal bovine serum (FBS) and antibiotics (penicillin and streptomycin) at 37°C and 5% CO_2. MSCs and BMSCs were treated with 20 μM YS49 (MedChemExpress, Monmouth Junction, NJ) as an activator of PI3K signaling for 1 day. We evaluated the responses of tumor cells and RAW264.7 cells to the application of 1–10 μg/mL recombinant Hsp90ab1 (OPCA05157; Aviva System Biology, San Diego), β-actin, and Myh9 (MBS717418, MBS717396; MyBioSource, San Diego, CA).

For *in vitro* and *ex vivo* assays, CM from 1×10^6 MSCs was collected and centrifuged at 2,000 rpm for 10 min. For *in vivo* experiments, serum-free CM was generated. MSC-derived CM was centrifuged at 2,000 rpm for 10 min and at 4,000 rpm for 10 min, followed by the filtration with a 0.22-μm polyethersulfone membrane (Sigma). We removed the remaining cell debris by the centrifugation at 10,000×*g* for 30 min at 4°C and exosomes by the ultra-centrifugation at 100,000×*g* (Type 90 Ti Rotor, Beckman, Brea, CA) overnight at 4°C. Using a buffer exchange filter (3 kD cut off; Amicon, Sigma), the supernatant was condensed approximately 10-fold (the final protein concentration adjusted to 1 mg/mL).

Differentiation of osteoclasts

The differentiation assay was conducted using RAW264.7 pre-osteoclasts in a 12-well plate.[44] We added 40 ng/mL RANKL to the culture medium, which was exchanged once on day 4. Using a tartrate-resistant acid phosphate (TRAP) staining kit (Sigma), adherent cells on the plate surface were stained on day 6. We identified TRAP-positive multinucleated cells with more than three nuclei as mature osteoclasts.

MTT, EdU, transwell invasion, and scratch assays

In the MTT assay, approximately 2,000 tumor cells were grown in 96-well plates on day 1. The described CM with and without recombinant proteins was applied on day 2, and tumor cells were stained

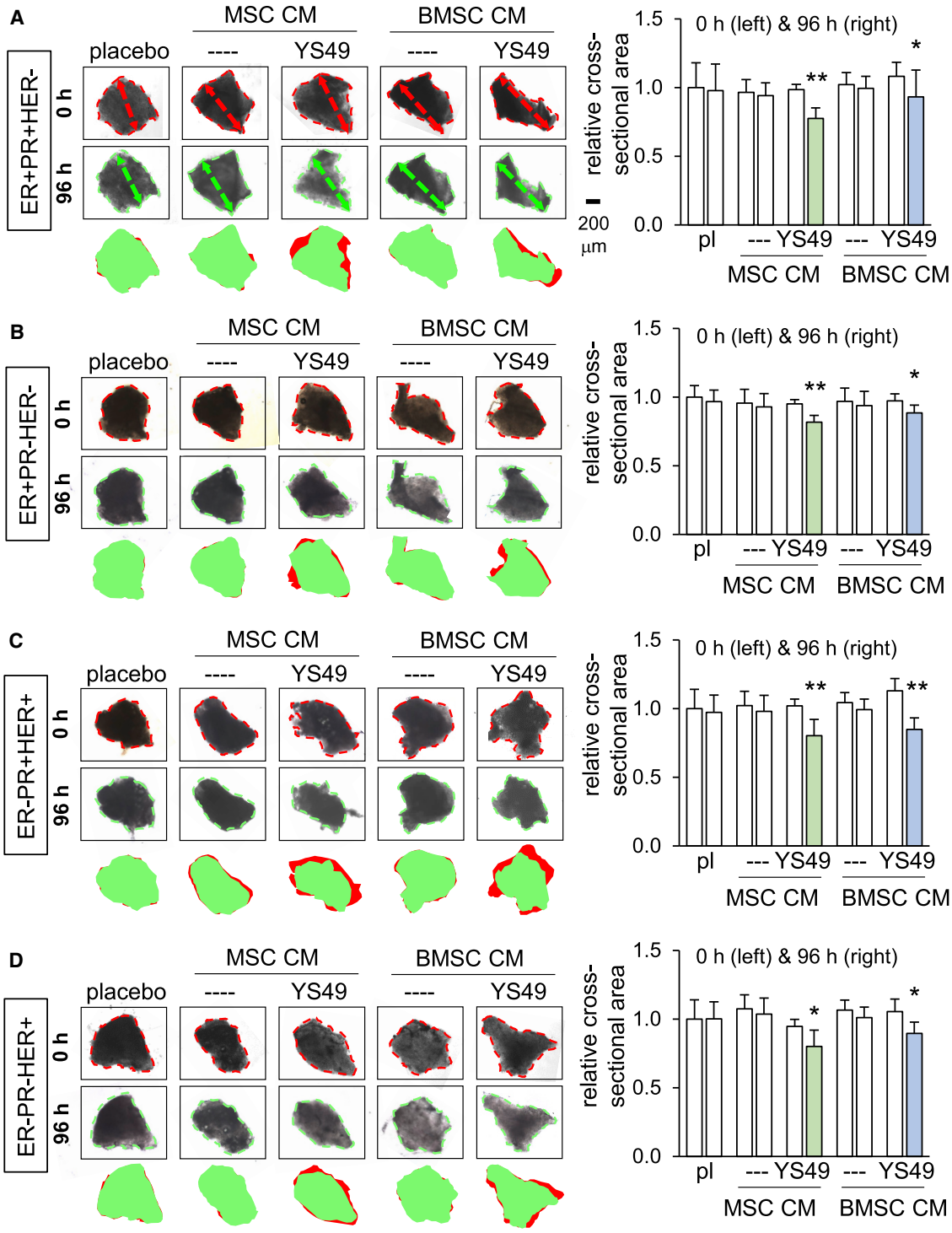

Figure 6. Shrinkage of human breast cancer tissue fragments by YS49 MSC/BMSC CM

(A–D) Images and the relative cross-sectional areas for the tissue with ER+/PR+/HER–. ER+/PR–/HER–. ER–/PR+/HER+, and ER–/PR–/HER+, respectively. *$p < 0.05$ and **$p < 0.01$.

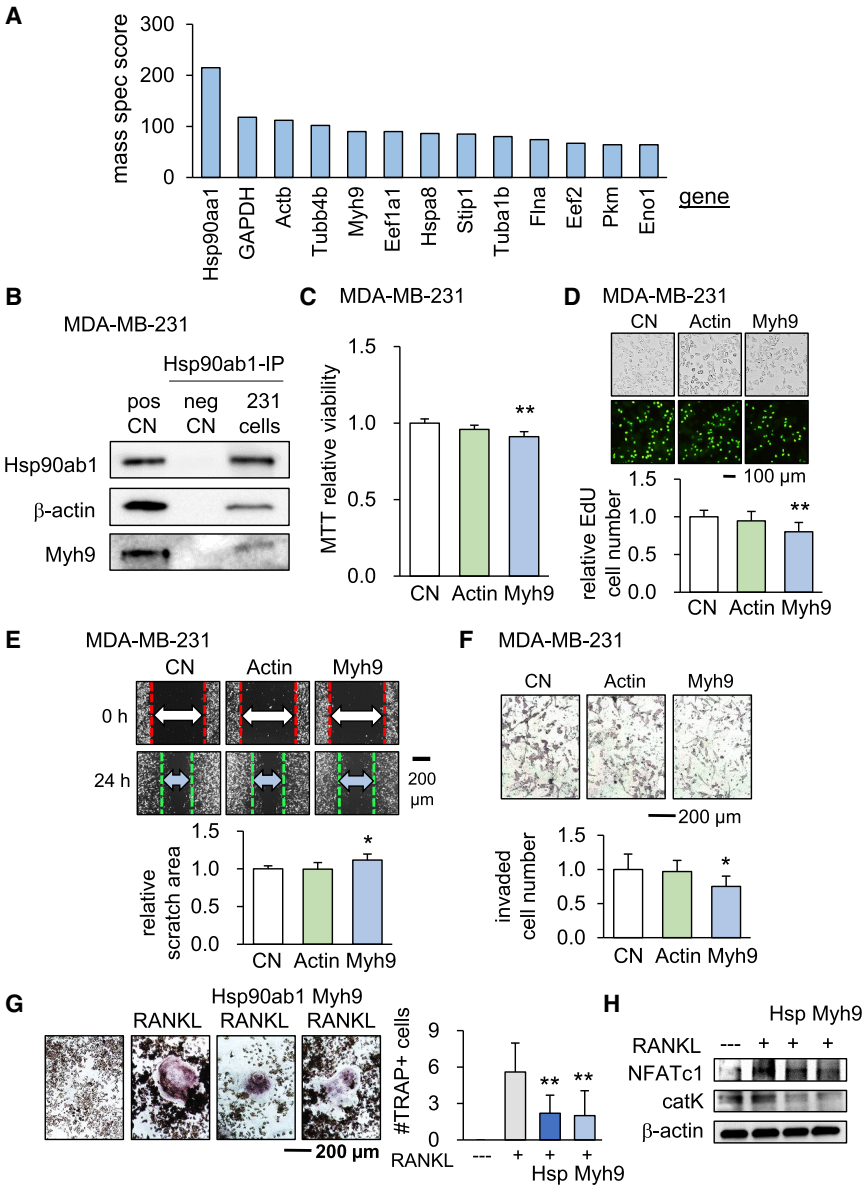

Figure 7. Hsp90ab1 and non-muscle myosin, Myh9, as an inhibitor of tumor progression and osteoclast development

(A) List of proteins that interact with Hsp90ab1, including β-actin and non-muscle myosin, Myh9. (B) Co-immunoprecipitation of β-actin and Myh9 with Hsp90ab1 in the protein extracts from the MDA-MB-231 ECM. (C–F) Reduction in MTT viability, EdU cell proliferation, two-dimensional motility, and cross-membrane invasion of MDA-MB-231 cells by recombinant Myh9 proteins. (G) Inhibition of the multinucleation of RANKL-stimulated RAW264.7 cells by recombinant Hsp90ab1 and Myh9 proteins. (H) Downregulation of NFATc1 and cathepsin K (cat K) by recombinant Hsp90ab1 and Myh9 proteins. CN, control, pos CN, positive control, and neg CN, negative control. *$p < 0.05$ and **$p < 0.01$.

using 0.5 mg/mL thiazolyl blue tetrazolium bromide (M5655, Sigma) on day 4. Optical density was determined at 570 nm for assessing metabolic activities. Using an absorbance ratio of each sample to control, the relative MTT value (metabolic activity) was assigned. In the EdU assay, the proliferation of tumor cells was evaluated using a fluorescence-based EdU kit (Click-iT EdU Alexa Fluor 488 imaging kit; ThermoFisher Scientific, Waltham, MA). We used eight images in total from four wells per group. Using the procedures previously described,[45] we also conducted the transwell invasion assay to detect the cell's invasive ability, in which invasion capacity was determined based on six randomly chosen images of the transwell membrane. In the wound-healing scratch assay, we evaluated the two-dimensional motility of tumor cells by determining the scratch areas of eight images per group.[46]

Ex vivo breast cancer assay

The Indiana University Institutional Review Board approved the use of human breast cancer tissue, which was received from the Indiana University Simon Comprehensive Cancer Center Tissue Procurement and Distribution Core. Small tissue fragments (0.5–0.8 mm in length) were manually generated from a surgically removed tissue sample (100–300 mg) using a scalpel. They were maintained in DMEM with 10% FBS and antibiotics on day 1. YS49 MSC/BMSC CM was given on day 2 for 2 additional days. Two-dimensional images of the fragments were taken on the first and last days and the difference in their size was blindly quantified.

Western blot analysis

Using a RIPA buffer with protease and phosphatase inhibitors (PIA32963, ThermoFisher Scientific, and 2006643, Calbiochem, Billerica, MA, respectively), cells were lysed. SDS gels (10%–15%) were used to size-fractionate proteins, followed by an electrotransfer to transfer membranes (IPVH00010, Millipore, Billerica, MA). The membrane was blocked for 1 h with a blocking buffer (1706404, Bio-Rad, Hercules, CA) and incubated with primary antibodies followed by horseradish peroxidase-conjugated secondary antibodies (7074/7076, Cell Signaling, Danvers, MA). Antibodies, used in this study were NFATc1, cathepsin K (Santa Cruz Biotechnology, Dallas, TX), Hsp90ab1 (Abcam, Cambridge, UK), Myh9 (3403S, Cell Signaling), and β-actin as a control (A5441, Sigma). A SuperSignal west femto maximum sensitivity substrate (PI34096, ThermoFisher Scientific) was used to visualize protein bands with a luminescent image analyzer (LAS-3000, Fuji Film, Tokyo, Japan).[47]

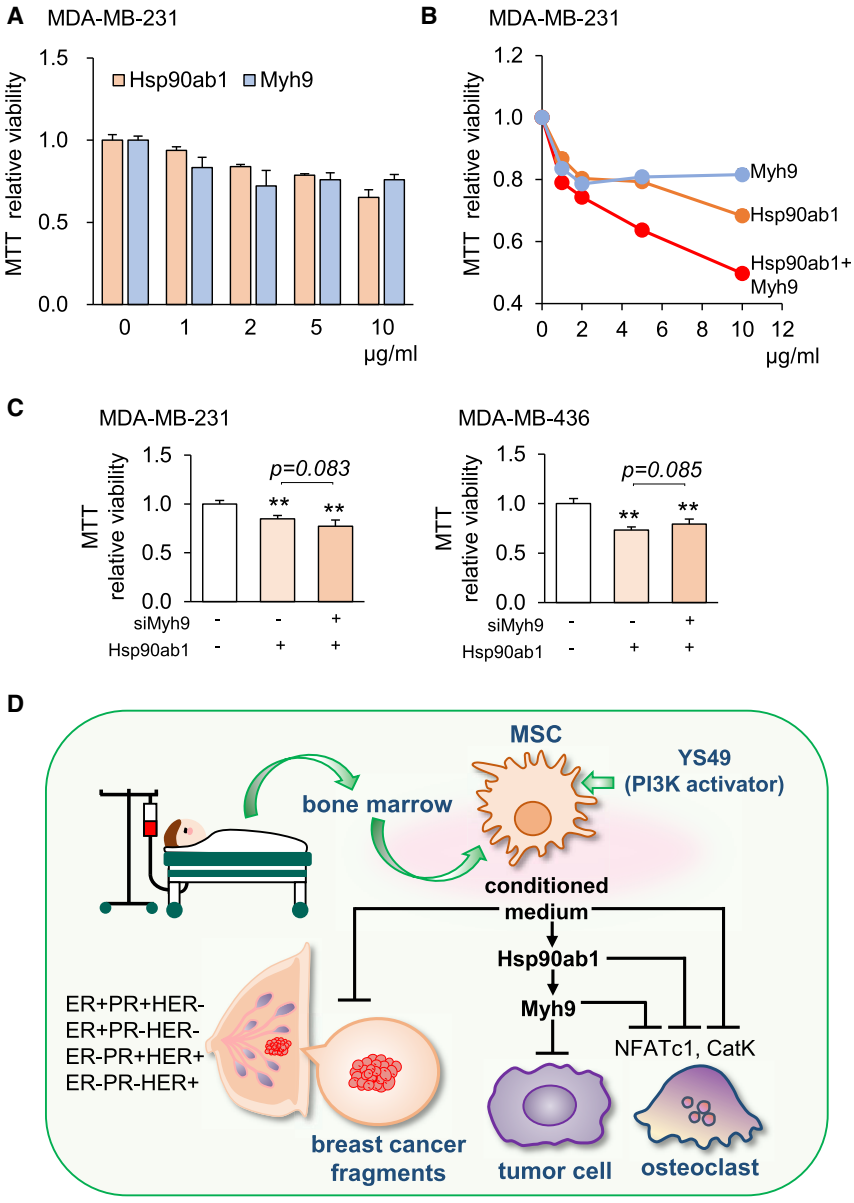

Figure 8. Tumor-suppressing effects of Hsp90ab1 and Myh9

(A, B) Reduction in MTT-based viability of MDA-MB-231 cells by recombinant Hsp90ab1 and Myh9 proteins. (C) Reduction in MTT viability of MDA-MB-231 and 436 breast cancer cells by recombinant Hsp90ab1 with or without silencing Myh9. (D) Proposed mechanism of the tumor-suppressive action of YS49 MSC CM via Hsp90ab1 and Myh9. **$p < 0.01$.

Plasmid transfection and RNA silencing

Using the procedure previously described,[45] Akt plasmids (#10841, Addgene, Watertown, MA), as well as a blank plasmid vector (FLAG-HA-pcDNA3.1, Addgene) as control, were transfected to MSCs and BMSCs. Using siRNA specific to Myh9 (s70266, ThermoFisher Scientific), we conducted RNA interference conducted using a negative siRNA (Silencer Select #1, ThermoFisher Scientific) as a nonspecific control.

Immunoprecipitation

Agarose beads were conjugated with protein A and rabbit IgG, and they were incubated with protein samples. Immunoprecipitation was conducted using the beads conjugated with anti-Hsp90ab1 antibody (R&D Systems). We collected the beads by centrifugation. Immunoprecipitated proteins were collected after washing the beads three times with PBS and western blotting analysis was conducted to evaluate immunoprecipitated proteins.

Mass spectrometry-based whole-genome proteomics

Using the protein samples that were immunoprecipitated with Hsp90ab1 in YS49 MSC CM, mass spectrometry-based whole-genome proteomics was conducted using the procedure previously described.[48,49] We used the Dionex UltiMate 3000 RSLC nano-system and the Q-exactive high-field hybrid quadrupole orbitrap mass spectrometer (ThermoFisher Scientific). We used MS/MS counts to quantify relative protein levels and focused on proteins that had at least 2 MS/MS counts with one or more unique peptides.

Animal models for mammary tumors and lung metastasis

The protocol SC292R was approved by the Indiana University Animal Care and Use Committee. The approved protocol complied with the Guiding Principles in the Care and Use of Animals endorsed by the American Physiological Society. Mice in this study were housed five per cage and provided with water and mouse chow ad libitum. In the mouse model of a mammary tumor, NOD/SCID/γ(−/−) (NSG) female mice (approximately 8 weeks) were provided by the *In Vivo* Therapeutics Core of the Indiana University Simon Comprehensive Cancer Center (Indianapolis, IN).[50] Mice were blindly divided into three groups (placebo, YS49 MSC CM, and YS49 BMSC CM groups; eight mice per group). They received subcutaneous inoculation of MDA-MB-231 cells (3.0×10^5 cells, 50 μL PBS) to the right side of the second pair in the mammary fat pad on day 1. From day 2 to day 17, mice in the two treatment groups received a daily intravenous injection of YS49 MSC and BMSC CM (50 μL CM). The placebo mice received the same volume of PBS. The animals were sacrificed on day 18. Mammary tumors were isolated and their weight was measured.

To evaluate the effect of YS49 MSC/BMSC CM on tumor invasion to the lung, we used three groups of NSG mice (approximately 8 weeks; placebo, YS49 MSC CM, and YS49 BMSC CM groups; 5 mice per group). As an intracardiac injection, MDA-MB-231 cells (approximately 3×10^5 cells in 100 μL PBS) were inoculated to all mice. The mice in the two treatment groups received YS49 MSC or BMSC CM, whereas mice in the placebo group were given a daily i.v. injection of PBS. Mice were sacrificed in 3 weeks for harvesting lungs and histological analysis was conducted. Harvested lungs were dehydrated using a series of graded alcohols, and they were embedded in paraffin after clearing in xylene. We sectioned the samples at 60-μm intervals and processed them using hematoxylin and eosin staining. We took images from five locations per slide and blindly quantified the tumor-invaded region as a ratio of the tumor-colonized area to the total area.[51,52]

Statistical analysis

Three or four independent experiments were conducted in cell culture studies, and the mean and standard deviation were determined. The sample size in the animal experiments was chosen to achieve a power of 80% with p value of less than 0.05. We selected tumor weight as the primary experimental outcome in the mammary tumor experiment, while the tumor-colonized area in the lung invasion experiment. One-way analysis of variance was used to evaluate statistical significance, while post hoc comparisons were performed using Bonferroni correction with the control group. We used the single and double asterisks to indicate $p < 0.05$ and $p < 0.01$, respectively, in the figures.

DATA AVAILABILITY

All data are available in the main text or supplemental information.

SUPPLEMENTAL INFORMATION

Supplemental information can be found online at https://doi.org/10.1016/j.omto.2022.08.003.

ACKNOWLEDGMENTS

The authors thank the Indiana University Simon Comprehensive Cancer Center for the use of the Tissue Procurement & Distribution Core, which provided breast cancer tissues. The authors also appreciate Hudie Li and Hailan Ma for their technical support.

AUTHOR CONTRIBUTIONS

B.Y.L. and H.Y. conceived the study and designed the experiments. X.S., K.L., U.K.A., and H.Y. collected, analyzed, and interpreted the data. X.S. and H.Y. drafted the manuscript.

DECLARATION OF INTERESTS

The authors declare no conflict of interest.

REFERENCES

1. Berman, A.T., Thukral, A.D., Hwang, W.T., Solin, L.J., and Vapiwala, N. (2013). Incidence and patterns of distant metastases for patients with early-stage breast cancer after breast conservation treatment. Clin. Breast Cancer *13*, 88–94.

2. Hess, K.R., Varadhachary, G.R., Taylor, S.H., Wei, W., Raber, M.N., Lenzi, R., and Abbruzzese, J.L. (2006). Metastatic patterns in adenocarcinoma. Cancer *106*, 1624–1633.

3. Liu, S., Sun, X., Li, K., Zha, R., Feng, Y., Sano, T., Dong, C., Liu, Y., Aryal, U.K., Sudo, A., et al. (2021). Generation of the tumor-suppressive secretome from tumor cells. Theranostics *11*, 8517–8534.

4. Liu, S., Wu, D., Sun, X., Fan, Y., Zha, R., Jalali, A., Feng, Y., Li, K., Sano, T., Vike, N., et al. (2021). Overexpression of Lrp5 enhanced the anti-breast cancer effects of osteocytes in bone. Bone Res. *9*, 32.

5. Sun, X., Li, K., Zha, R., Liu, S., Fan, Y., Wu, D., Hase, M., Aryal, U.K., Lin, C.C., Li, B.Y., and Yokota, H. (2021). Preventing tumor progression to the bone by induced tumor-suppressing MSCs. Theranostics *11*, 5143–5159.

6. Liu, S.-Z., Sun, X., Li, K.-X., Lin, C.-C., Na, S., Li, B.-Y., and Yokota, H. (2021). Tumor cell secretomes in response to anti- and pro-tumorigenic agents. Onco *1*, 101–113.

7. Tung, K.H., Ernstoff, M.S., Allen, C., and Shu, S.L. (2019). A Review of exosomes and their role in the tumor microenvironment and host-tumor "macroenvironment". J. Immunol. Sci. *3*, 4–8.

8. Madden, E.C., Gorman, A.M., Logue, S.E., and Samali, A. (2020). Tumour cell secretome in chemoresistance and tumour recurrence. Trends Cancer *6*, 489–505.

9. Pavlou, M.P., and Diamandis, E.P. (2010). The cancer cell secretome: a good source for discovering biomarkers? J. Proteomics *73*, 1896–1906.

10. Wu, T., and Dai, Y. (2017). Tumor microenvironment and therapeutic response. Cancer Lett. *387*, 61–68.

11. Yao, L., Zhang, Y., Chen, K., Hu, X., and Xu, L.X. (2011). Discovery of IL-18 as a novel secreted protein contributing to doxorubicin resistance by comparative secretome analysis of MCF-7 and MCF-7/Dox. PLoS One *6*, e24684.

12. Wu, J.Y., Huang, T.W., Hsieh, Y.T., Wang, Y.F., Yen, C.C., Lee, G.L., Yeh, C.C., Peng, Y.J., Kuo, Y.Y., Wen, H.T., et al. (2020). Cancer-derived succinate promotes macrophage polarization and cancer metastasis via succinate receptor. Mol. Cell *77*, 213–227.e5.

13. López de Andrés, J., Griñán-Lisón, C., Jiménez, G., and Marchal, J.A. (2020). Cancer stem cell secretome in the tumor microenvironment: a key point for an effective personalized cancer treatment. J. Hematol. Oncol. *13*, 136.

14. Cebrián, M.J.G., Bauden, M., Andersson, R., Holdenrieder, S., and Ansari, D. (2016). Paradoxical role of HMGB1 in pancreatic cancer: tumor suppressor or tumor promoter? Anticancer. Res. *36*, 4381–4389.

15. Kanda, H., and Igaki, T. (2020). Mechanism of tumor-suppressive cell competition in flies. Cancer Sci. *111*, 3409–3415.

16. Nagata, R., Nakamura, M., Sanaki, Y., and Igaki, T. (2019). Cell competition is driven by autophagy. Dev. Cell *51*, 99–112.e4.

17. Amoyel, M., and Bach, E.A. (2014). Cell competition: how to eliminate your neighbours. Development *141*, 988–1000.

18. Li, K.X., Sun, X., Li, B.Y., and Yokota, H. (2021). Conversion of osteoclasts into bone-protective, tumor-suppressing cells. Cancers (Basel) *13*, 5593.

19. de Girolamo, L., Lucarelli, E., Alessandri, G., Avanzini, M.A., Bernardo, M.E., Biagi, E., Brini, A.T., D'Amico, G., Fagioli, F., Ferrero, I., et al. (2013). Mesenchymal stem/stromal cells: a new "cells as drugs" paradigm. Efficacy and critical aspects in cell therapy. Curr. Pharm. Des. *19*, 2459–2473.

20. Hass, R., and Otte, A. (2012). Mesenchymal stem cells as all-round supporters in a normal and neoplastic microenvironment. Cell Commun. Signal. *10*, 26.

21. Melzer, C., Yang, Y., and Hass, R. (2016). Interaction of MSC with tumor cells. Cell Commun. Signal. *14*, 20.

22. He, N., Kong, Y., Lei, X., Liu, Y., Wang, J., Xu, C., Wang, Y., Du, L., Ji, K., Wang, Q., et al. (2018). MSCs inhibit tumor progression and enhance radiosensitivity of breast cancer cells by down-regulating Stat3 signaling pathway. Cell Death Dis. *9*, 1026.

23. Zhu, Y., Sun, Z., Han, Q., Liao, L., Wang, J., Bian, C., Li, J., Yan, X., Liu, Y., Shao, C., and Zhao, R.C. (2009). Human mesenchymal stem cells inhibit cancer cell proliferation by secreting DKK-1. Leukemia *23*, 925–933.

24. Wang, H., Deng, G., Ai, M., Xu, Z., Mou, T., Yu, J., Liu, H., Wang, S., and Li, G. (2019). Hsp90ab1 stabilizes LRP5 to promote epithelial-mesenchymal transition via

activating of AKT and Wnt/β-catenin signaling pathways in gastric cancer progression. Oncogene *38*, 1489–1507.

25. Haase, M., and Fitze, G. (2016). HSP90AB1: helping the good and the bad. Gene *575*, 171–186.
26. Suzuki, S., and Kulkarni, A.B. (2010). Extracellular heat shock protein HSP90beta secreted by MG63 osteosarcoma cells inhibits activation of latent TGF-beta1. Biochem. Biophys. Res. Commun. *398*, 525–531.
27. Taipale, M., Jarosz, D.F., and Lindquist, S. (2010). HSP90 at the hub of protein homeostasis: emerging mechanistic insights. Nat. Rev. Mol. Cell Biol. *11*, 515–528.
28. Li, Y.R., and Yang, W.X. (2016). Myosins as fundamental components during tumorigenesis: diverse and indispensable. Oncotarget *7*, 46785–46812.
29. Pecci, A., Ma, X., Savoia, A., and Adelstein, R.S. (2018). MYH9: structure, functions and role of non-muscle myosin IIA in human disease. Gene *664*, 152–167.
30. Wang, Y., Liu, S., Zhang, Y., and Yang, J. (2019). Myosin heavy chain 9: oncogene or tumor suppressor gene? Med. Sci. Monit. *25*, 888–892.
31. Dai, X., Xiang, L., Li, T., and Bai, Z. (2016). Cancer hallmarks, biomarkers and breast cancer molecular subtypes. J. Cancer *7*, 1281–1294.
32. Sun, X., Li, K., Hase, M., Zha, R., Feng, Y., Li, B.Y., and Yokota, H. (2022). Suppression of breast cancer-associated bone loss with osteoblast proteomes via Hsp90ab1/moesin-mediated inhibition of TGFβ/FN1/CD44 signaling. Theranostics *12*, 929–943.
33. Backe, S.J., Sager, R.A., Woodford, M.R., Makedon, A.M., and Mollapour, M. (2020). Post-translational modifications of Hsp90 and translating the chaperone code. J. Biol. Chem. *295*, 11099–11117.
34. Zhang, G., Liu, Z., Ding, H., Zhou, Y., Doan, H.A., Sin, K.W.T., Zhu, Z.J., Flores, R., Wen, Y., Gong, X., et al. (2017). Tumor induces muscle wasting in mice through releasing extracellular Hsp70 and Hsp90. Nat. Commun. *8*, 589.
35. Li, K., Sun, X., Zha, R., Liu, S., Feng, Y., Sano, T., Aryal, U.K., Sudo, A., Li, B.Y., and Yokota, H. (2022). Counterintuitive production of tumor-suppressive secretomes from Oct4- and c-Myc-overexpressing tumor cells and MSCs. Theranostics *12*, 3084–3103.
36. Birbo, B., Madu, E.E., Madu, C.O., Jain, A., and Lu, Y. (2021). Role of HSP90 in cancer. Int. J. Mol. Sci. *22*, 10317.
37. Zhong, Y., Long, T., Gu, C.S., Tang, J.Y., Gao, L.F., Zhu, J.X., Hu, Z.Y., Wang, X., Ma, Y.D., Ding, Y.Q., et al. (2021). MYH9-dependent polarization of ATG9B promotes colorectal cancer metastasis by accelerating focal adhesion assembly. Cell Death Differ. *28*, 3251–3269.
38. Vasan, N., Baselga, J., and Hyman, D.M. (2019). A view on drug resistance in cancer. Nature *575*, 299–309.
39. Dai, R., Wu, Z., Chu, H.Y., Lu, J., Lyu, A., Liu, J., and Zhang, G. (2020). Cathepsin K: the action in and beyond bone. Front. Cell Dev. Biol. *8*, 433.
40. Kim, J.H., and Kim, N. (2014). Regulation of NFATc1 in osteoclast differentiation. J. Bone Metab. *21*, 233–241.
41. Maurizi, A., and Rucci, N. (2018). The osteoclast in bone metastasis: player and target. Cancers (Basel) *10*, E218.
42. Oryan, A., Kamali, A., Moshiri, A., and Baghaban Eslaminejad, M. (2017). Role of mesenchymal stem cells in bone regenerative medicine: what is the evidence? Cells Tissues Organs *204*, 59–83.
43. Kumar, B., Prasad, M., Bhat-Nakshatri, P., Anjanappa, M., Kalra, M., Marino, N., Storniolo, A.M., Rao, X., Liu, S., Wan, J., et al. (2018). Normal breast-derived epithelial cells with luminal and intrinsic subtype-enriched gene expression document interindividual differences in their differentiation cascade. Cancer Res. *78*, 5107–5123.
44. Cuetara, B.L.V., Crotti, T.N., O'Donoghue, A.J., and McHugh, K.P. (2006). Cloning and characterization of osteoclast precursors from the RAW264.7 cell line. In Vitro Cell. Dev. Biol. Anim. *42*, 182–188.
45. Liu, S., Fan, Y., Chen, A., Jalali, A., Minami, K., Ogawa, K., Nakshatri, H., Li, B.Y., and Yokota, H. (2018). Osteocyte-driven downregulation of snail restrains effects of Drd2 inhibitors on mammary tumor cells. Cancer Res. *78*, 3865–3876.
46. Liu, S., Liu, Y., Minami, K., Chen, A., Wan, Q., Yin, Y., Gan, L., Xu, A., Matsuura, N., Koizumi, M., et al. (2018). Inhibiting checkpoint kinase 1 protects bone from bone resorption by mammary tumor in a mouse model. Oncotarget *9*, 9364–9378.
47. Takigawa, S., Frondorf, B., Liu, S., Liu, Y., Li, B., Sudo, A., Wallace, J.M., Yokota, H., and Hamamura, K. (2016). Salubrinal improves mechanical properties of the femur in osteogenesis imperfecta mice. J. Pharmacol. Sci. *132*, 154–161.
48. Connelly, K.E., Hedrick, V., Paschoal Sobreira, T.J., Dykhuizen, E.C., and Aryal, U.K. (2018). Analysis of human nuclear protein complexes by Quantitative mass spectrometry profiling. Proteomics *18*, e1700427.
49. Opoku-Temeng, C., Onyedibe, K.I., Aryal, U.K., and Sintim, H.O. (2019). Proteomic analysis of bacterial response to a 4-hydroxybenzylidene indolinone compound, which re-sensitizes bacteria to traditional antibiotics. J. Proteomics *202*, 103368.
50. Pham, P.V., Le, H.T., Vu, B.T., Pham, V.Q., Le, P.M., Phan, N.L.C., Trinh, N.V., Nguyen, H.T.L., Nguyen, S.T., Nguyen, T.L., and Phan, N.K. (2016). Targeting breast cancer stem cells by dendritic cell vaccination in humanized mice with breast tumor: preliminary results. Onco. Targets Ther. *9*, 4441–4451.
51. Li, J., Zeng, T., Li, W., Wu, H., Sun, C., Yang, F., Yang, M., Fu, Z., and Yin, Y. (2020). Long non-coding RNA SNHG1 activates HOXA1 expression via sponging miR-193a-5p in breast cancer progression. Aging (Albany NY) *12*, 10223–10234.
52. Xiao, Y., Cong, M., Li, J., He, D., Wu, Q., Tian, P., Wang, Y., Yang, S., Liang, C., Liang, Y., et al. (2021). Cathepsin C promotes breast cancer lung metastasis by modulating neutrophil infiltration and neutrophil extracellular trap formation. Cancer Cell. *39*, 423–437.e7.